International Journal of Mass Spectrometry 286 (2009) 89–94

Contents lists available at ScienceDirect

International Journal of Mass Spectrometry

journal homepage: www.elsevier.com/locate/ijms

Tandem RF-only quadrupole mass filter with quadrupolar excitation

Gongyu Jiang [a], Chan Luo [a], N.V. Konenkov [b], Chuan-Fan Ding [a,*]

[a] Shanghai Key Laboratory of Molecular Catalysis and Innovative Materials, Department of Chemsitry, Fudan University, 220 Handan Road, Shanghai 200433, China
[b] Department of Physics and Mathematics, Ryazan State University, Svoboda, 46, Ryazan 390000, Russian Federation

ARTICLE INFO

Article history:
Received 4 February 2009
Received in revised form 2 July 2009
Accepted 6 July 2009
Available online 10 July 2009

Keywords:
Tandem RF-only quadrupole mass filter
High mass reject filter
Auxiliary quadrupolar excitation
Instability pass band
Separation time

ABSTRACT

We report the computer simulation results of a tandem RF-only quadrupole mass filter. This mass filter consists of two short quadrupole rod sets, Q1 and Q2. The first quadrupole, Q1, is operated as a higher mass reject filter to remove lower q ions. The main filter, Q2, is a RF-only quadrupole, and it is used to give suitable narrow pass band on q axis. Quadrupole excitation by additional RF voltage leads to instability bands along q axis between $q = 0$ and $q = 0.2$, and this instability band can be used to remove low q ions with $m = M_0 - \infty$ mass range. Quadrupole excitation creates a narrow pass band near $q_0 = 0.9080$ in Q2. $R_{0.1} = 1150$ could be achieved at short separation time $n = 40$ in Q2.

1. Introduction

Quadrupole mass filter is usually operated as a narrow pass band filter by applying both DC and RF voltages to the quadrupole electrodes, and the applied DC and RF voltages correspond to the values of Mathieu parameters a and q near the apex of the first stability diagram [1]. The resolution power is adjusted by changing the slope of scan line $a = 2\lambda q$; $\lambda = U/V$ is the scan slope. Under this operation mode, the quality of the quadrupole field is determined by both mechanical tolerance of the rods set and the stability of RF/DC voltage. The DC and RF power supply is generally more complex than the RF-only power supply.

Brinkman in 1972 [2] described the RF-only operation of a quadrupole mass filter. Richards et al. [3] discussed the possibility of such operation on QMF with rectangular wave form power supply. Leck and co-workers [4–8] studied RF-only separation mode and achieved remarkable results. However, the practical application of RF-only QMF remains very challenging due to the high background noise created by the high mass to charge ions.

To overcome the background noise and understand the mechanism of ion mass separation, Hager and Londry [9] investigated the fringing field effect in detail and reported that the ions near $q = 0.907$ become unstable and gain large radial amplitude. In the output fringing region, part of radial energy is transformed into axial energy. The more unstable ions are in radial direction, the more axial energy they gain. The unstable ions with well-defined axial energies and discrete charges are therefore distinguished from those with stable trajectories by energy filters and similar devices. In order to remove lower q ions (higher ion mass with stable trajectories), Hager proposed to use ±15% RF unbalance voltages and ±3 V resolving DC on opposite electrode pairs [10]. Such method substantially reduced background noise and created high performance linear ion trap with axial ion ejection [11].

Du and Douglas [12] described a tandem quadrupole mass filter arrangement. In order to improve mass peak shape, they used two quadrupole mass filter with a small mass offset between them. The resolution of the tandem analyzer can be adjusted by changing the mass offset.

Here we report the computer simulation results of a tandem RF-only quadrupole mass filter of two short quadrupole rod sets, Q1 and Q2. The first quadrupole, Q1, is operated as a higher mass reject filter to remove lower q ions. We used parametric resonance quadrupole excitation of ion vibrations by auxiliary low frequency RF voltage with small amplitude [13–15]. The main filter, Q2, is a RF-only quadrupole [9], and it was used to gives suitable narrow pass band on q axis. Q2 is also called quadrupole with auxiliary RF voltage [14] and quadrupole with amplitude modulation [16]. Recently, operation of RF-only mass spectrometer with auxiliary excitation was reported [17], and it used swift wave excitation of most mass-to-charge (m/z) ions to transmit a few selected m/z ions. This method differs substantially from our approach.

* Corresponding author. Tel.: +86 21 556664549; fax: +86 21 556664549.
E-mail address: cfding@fudan.edu.cn (C.-F. Ding).

1387-3806/$ – see front matter © 2009 Elsevier B.V. All rights reserved.
doi:10.1016/j.ijms.2009.07.001

2. Simulations results

2.1. High mass reject filter with auxiliary quadrupole excitation

The operation of high mass reject filter is based on parametric quadrupolar resonance excitation of ion vibrations, which is created by an additional RF voltage applied to the QMF electrodes [14–16]. The ion motion equations for such two harmonic RF fields are [16]:

$$\frac{d^2x}{d\xi^2} - [2q\cos 2(\xi - \xi_0) + 2q'\cos 2\nu(\xi - \xi_0)]x = 0 \quad (1)$$

$$\frac{d^2y}{d\xi^2} + [2q\cos 2(\xi - \xi_0) + 2q'\cos 2\nu(\xi - \xi_0)]y = 0 \quad (2)$$

$$\text{Here } q = \frac{4eV}{m\Omega^2 r_0^2},\ \xi = \frac{\Omega t}{2},\ q' = \frac{4eV'}{m\Omega^2 r_0^2},\ \nu = \frac{\omega}{\Omega} \quad (3)$$

e is the ion charge, m the ion mass, V the amplitude of the main RF voltage (from ground to peak), Ω the angular frequency of the RF voltage, V' and ω the amplitude and the angular frequency of the auxiliary RF voltage, ξ_0 the initial RF phase, and x and y transverse quadrupole directions.

When $\nu = k/P$ is simple ratio and $k < P$, the instability pass bands on the q axis are located near β values of $1/P$, $2/P$, ..., $(P-1)/P$ [13,15]. More powerful instability bands are located near the original stability boundaries at $q = 0$ and $q = 0.908$ and $\beta = 1/P$ and $\beta = (P-1)/P$.

The ion transmissions T, dependent on parameter q, are shown in Fig. 1(a) for quadrupole with auxiliary lower frequency excitations. For each point at the transmission curve $T(q)$, $N = 2000$ ion trajectories were calculated. These ions were set at 20 initial RF phases $\xi_0 = 0, \pi/20, 2\pi/20, \ldots, 19\pi/20$, and for each initial RF phase Na = 100 ions were randomly distributed on an input circular aperture plate with radius $r_a = 0.3r_0$. r_0 is defined as the radius of the inscribed circle tangential to the inner surface of the electrodes. Initial transverse ion velocities were set to zero for comparing transmissions in different conditions. The ion separation time n, which equals to 60 here, is the number of RF cycles ions spent in the quadrupole field.

As shown in Fig. 1(a), there exists a powerful instability band near $\beta = \nu = 1/10$. When the auxiliary parameter q' (Eq. (3)) increases up to $q' = 0.02$, the instability band, which rejects the lower q ions with q from 0 to 0.2, is formed. Here we define the edge of the right instability band as q1. The left instability band $q = 0$ is not exactly an 'instability band' because it corresponds to ion mass $m = \infty$ according to Eq. (3). Thus, the higher mass ions may be removed from quadrupole field by parametric low frequency excitation of ion vibrations. With increasing q' value, as seen from the transmission curve, the resonance dips appear at stability parameters $\beta = 2/10$, 3/10, etc.

Fig. 1(b) shows the variation of transmission in correspondence to the changing separation time n. With increasing n, the edge of the instability band becomes sharper, but the overall shape remains the same.

Fig. 1(c) shows the transmission curves $T(q)$ for different input aperture radius $r_a = 0.1r_0$, ..., $0.8r_0$ and $n = 50$. The sizes of apertures do not have great influence on the edge of instability band, but they affect the ion transmission efficiency. The wider ions are distributed, the lower transmission efficiency is.

2.2. High mass reject filter with amplitude modulation

Quadrupole excitation by amplitude modulation of main RF drive voltage also leads to instability bands along q axis. The ion motion equations in quadrupole with amplitude field modulation

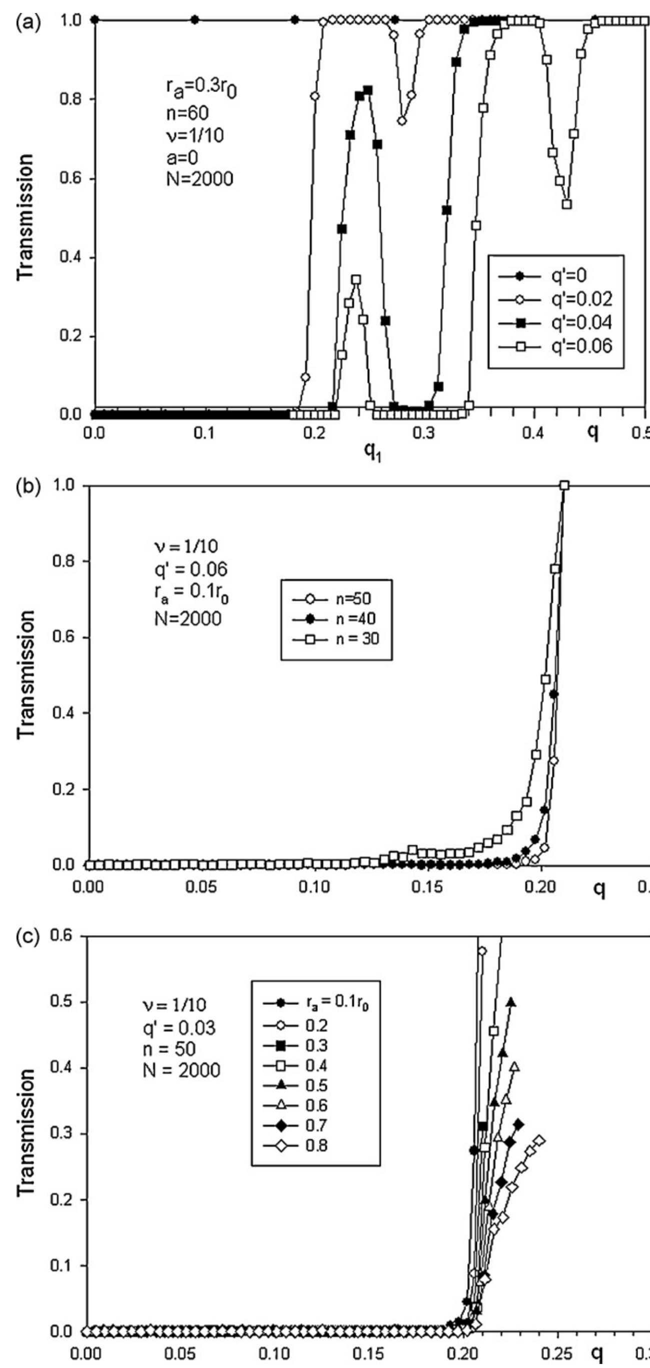

Fig. 1. (a) Transmission curves $T(q)$ for different excitation parameter $q' = 0$, 0.02, 0.04, 0.06. $r_a = 0.3r_0$ is radius of input aperture. $n = 60$ is number of RF cycles of ion motion integration. $\nu = \omega/\Omega = 1/10$ is the relative frequency ratio of auxiliary RF signal. $N = 2000$ is number of calculated trajectories per curve point. (b) Influence of separation time n on instability band edge with $r_a = 0.3r_0$, $\nu = \omega/\Omega = 1/10$, and $N = 2000$. (c) Right instability band edges at r_a from $0.1r_0$ to $0.8r_0$ and $n = 50$.

can be written as [16]:

$$\frac{d^2x}{dt^2} + 2q\cos 2(\xi - \xi_0)(1 + m\cos 2\nu(\xi - \xi_0))x = 0; \quad (4)$$

$$\frac{d^2y}{dt^2} - 2q\cos 2(\xi - \xi_0)(1 + m\cos 2\nu(\xi - \xi_0))y = 0; \quad (5)$$

Here q, ν and ξ are the same as in Eq. (3) and m is the modulation parameter. If $\nu = Q/P$ is a simple ratio and $Q < P$, the instability bands follow along $\beta = 1/P$, ..., $(P-1)/P$ stability parameters. Using previous ion trajectory simulation method, we calculated the

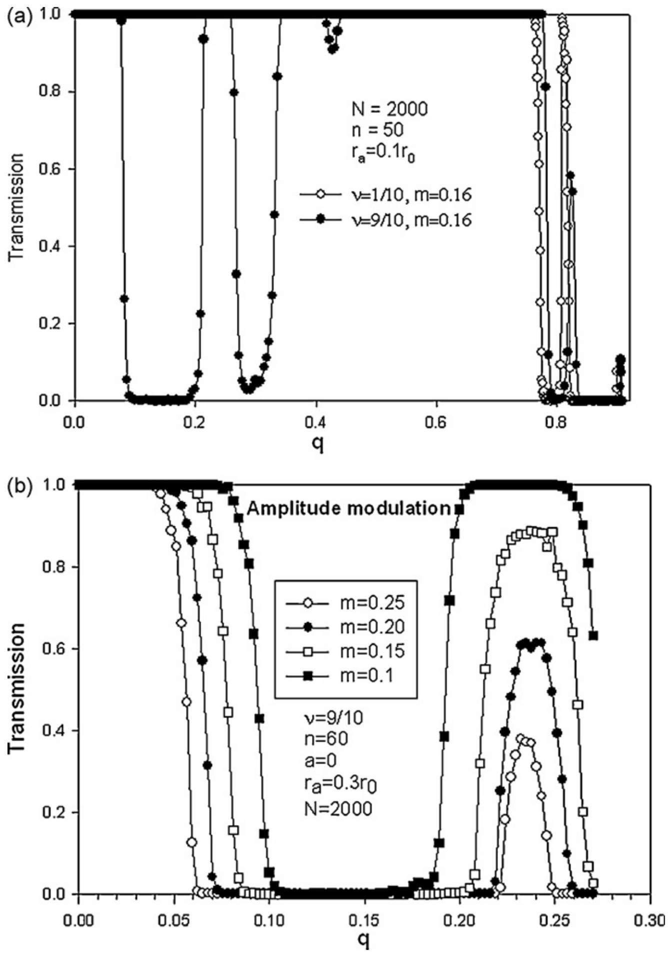

Fig. 2. (a) Transmission of a RF-only quadrupole mass filter with high ($\nu = 9/10$) and low ($\nu = 1/10$) frequency amplitude modulation. $n = 50$, $r_a = 0.1r_0$ and modulation parameter $m = 0.16$. (b) Influence of the modulation parameter m on instability band width near low q region at high frequency ($\nu = 9/10$) modulation.

transmission curves $T(q)$ by the numerical integration of ion motion Eqs. (4) and (5) for different modulation parameter values m and ν.

Fig. 2(a) shows the $T(q)$ curves of low ($\nu = 1/10$) and high ($\nu = 9/10$) modulation frequencies with parameters $m = 0.16$ at $n = 50$ and $r_a = 0.1r_0$. At high frequency auxiliary quadrupole excitation ($\nu = 9/10$), an obvious instability band is formed at low q values near $\beta = 1/10$; but at low modulation frequency ($\nu = 1/10$), the instability band disappear. The influence of the high frequency amplitude modulation depth m on the instability band width near low q values is illustrated in Fig. 2(b). With the m increasing to 0.25, the width

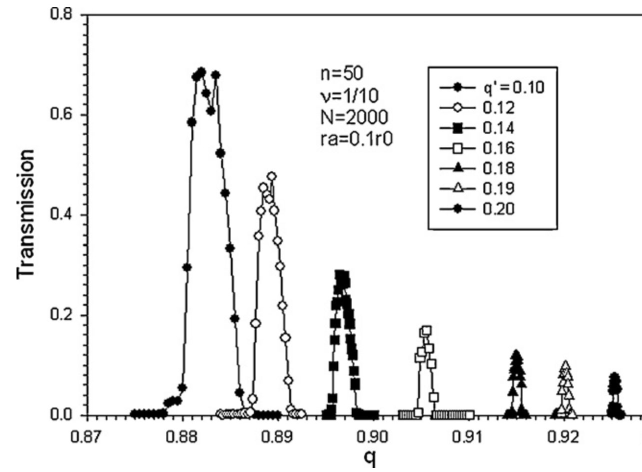

Fig. 4. Influence of the excitation parameter q' ion peak position on axis q and resolution power.

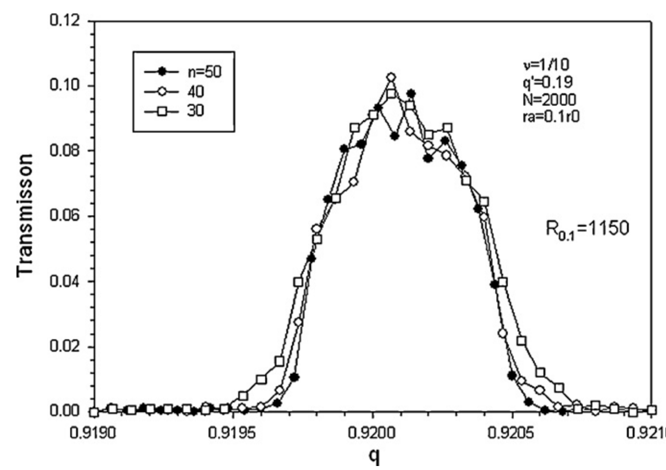

Fig. 5. Mass peak shape formed by quadrupole Q2 at relatively high resolution $R_{0.1} = 1150$ and different separation time $n = 30$, 40 and 50.

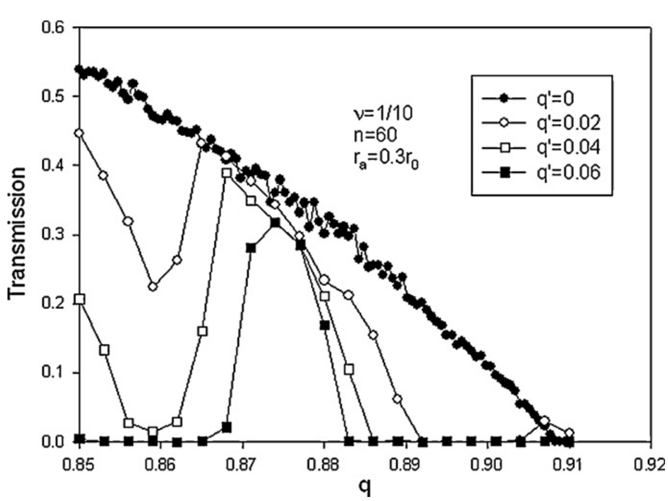

Fig. 3. Transmission of RF-only quadrupole Q2 with auxiliary low frequency $\nu = 1/10$ voltage and different excitation parameters $q' = 0.0$, 0.02, 0.04, 0.06.

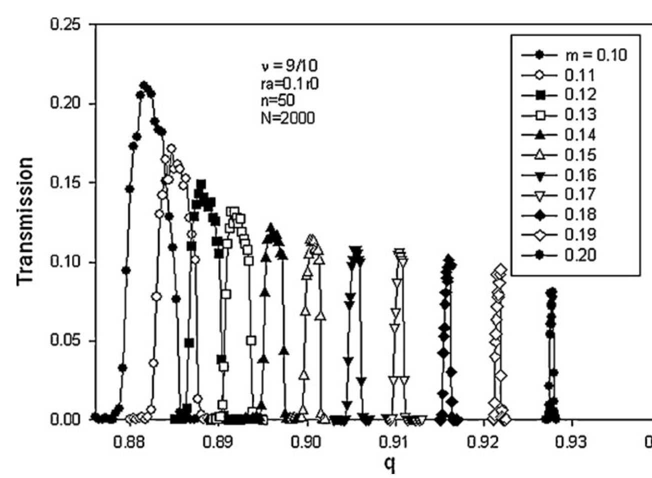

Fig. 6. Influence of the modulation parameter m on peak position along q axis and resolution power.

of instability band is increased to $\Delta q = 0.22 - 0.05 = 0.17$ but it still does not reach the lowest side $q = 0$. At the same time, the transmission of the ions with q greater than the right band of the instability band is rapidly reduced.

2.3. Mass filter with small stability islands formed by auxiliary quadrupole excitation

As mentioned before, $\beta = (P - 1)/P$ is the other strong instability band formed by auxiliary quadrupole excitation of driving RF voltage of the quadrupole mass filter. Fig. 3 shows the stability island created by auxiliary quadrupole excitation at $\beta = 9/10$ and $\nu = 1/10$. The transmission curves are simulated for different excitation parameter $q' = 0.0$, 0.02, 0.04 and 0.06. We found that the small stability island gradually appears along with an increasing q'. Here we define the left and right boundary of this stability island q2 and q3. As shown in Fig. 4, this stability island is moving right while q' is increasing. At the same time, the resolution is improving.

The influence of separation time n on peak shape at high resolution $R_{0.1} = 1150$ is shown in Fig. 5 with $q' = 0.19$. It can be seen that the resolution $R_{0.1} = 1150$ is achieved after ion passed through the rods for 40 RF cycles; longer rods (50 RF cycles) make mass peak slightly better.

2.4. Mass filter with small stability islands formed by amplitude modulation

Stability island is formed near boundary $q = 0.908$ when the amplitude modulation of the main drive RF voltage is used (Fig. 6). With an increasing m, the island is moving along q axis to the right, transmission is decreasing, and resolution is improving. Both auxiliary quadrupole excitation and amplitude modulation make the RF-only mass filter a narrow pass band filter.

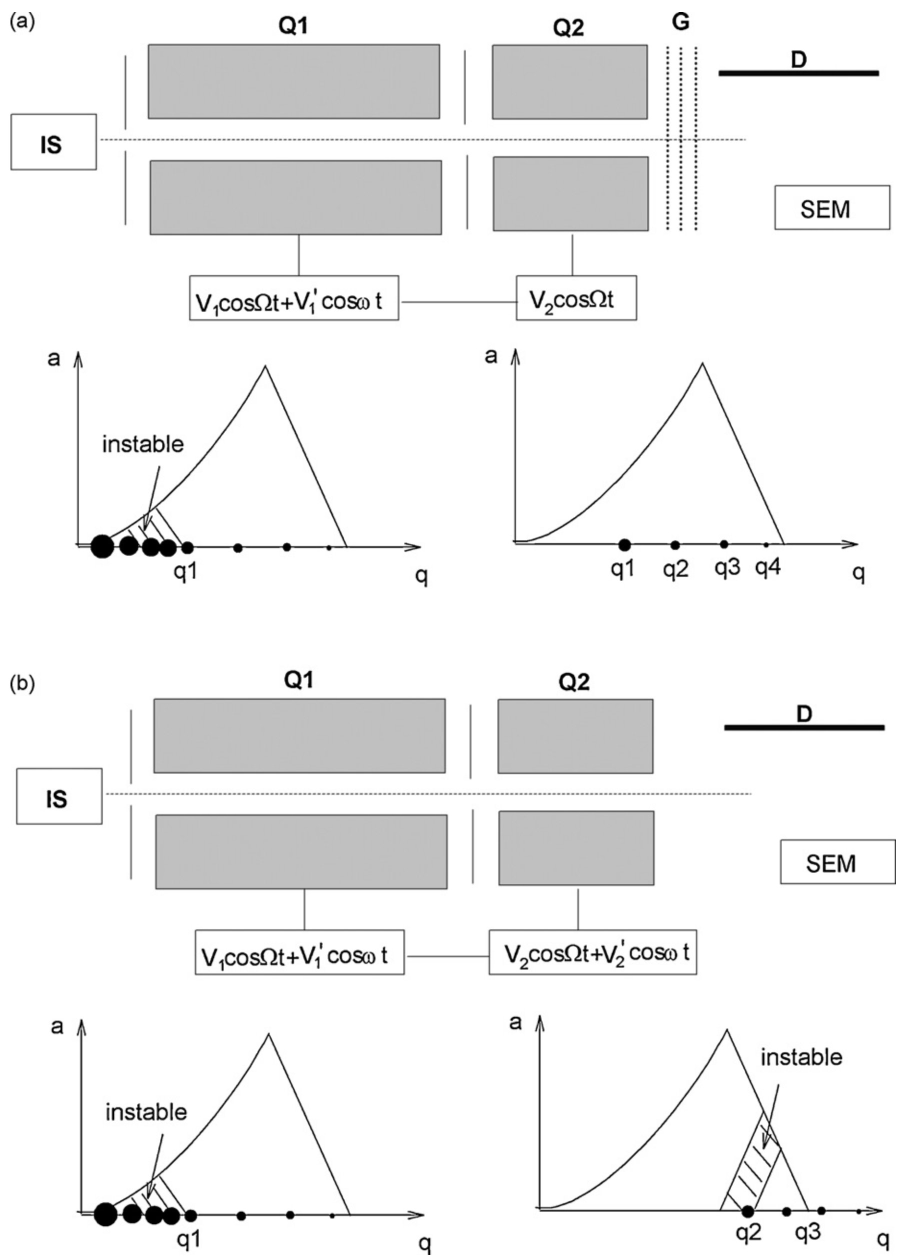

Fig. 7. Different configurations of the RF-only tandem mass filter. (a) First configuration of the RF-only tandem mass filter. IS is ion source, Q1 is reject high mass quadrupole, Q2 is mass selective filter operated near $q = 0.907$, G is greed energy filter, and SEM is ion detector. (b) Second configuration of the RF-only tandem mass filter. IS is ion source, Q1 is reject high mass quadrupole, Q2 is mass selective filter with narrow pass band, and SEM is ion detector.

2.5. *Configuration of tandem mass filters*

The tandem RF-only quadrupole mass filter consists of two quadrupole rod sets, Q1 and Q2. Q1 is working as a pre-mass filter to remove low q ions. Low background noise and high sensitivity are expected as all the high m/z ions are banished. Q2 is working as a mass filter that produces mass peaks.

According to simulation results, Q1 is an efficient high mass ions ejector. It needs only 40–50 RF cycles to build a sharp boundary and block high mass ions getting. Q1 does not need to be long, and 5 cm seems to be sufficient. With the help of Q1, the latter mass filter Q2 can work better. Here we give two examples of Q1 and Q2 under RF-only voltages.

2.5.1. *High mass reject filter and axial ion excitation mass filter*

Fig. 7(a) shows the configurations of Q1 working as a high mass reject filter and Q2 as an axial ion excitation mass filter. Let us define $\alpha = V2/V1$; V1, V2 are the amplitudes of the main driving RF of Q1, Q2 respectively. α remains constant in mass scanning. If $\alpha = 1$, all the ions with q value more than q1 pass through Q1 into Q2 for further analysis. If $\alpha > 1$, the q value of the stable ions running through Q1 is changing from q1 into q2, q3, q4 in Q2. By setting $\alpha > 1$, we can choose a continuous range of q value ions for analysis in axial ion excitation method.

As mentioned before, there are two ways to create an instability band. One is to choose q values between 0 and 0.2 using auxiliary quadrupole excitation method; the other is to choose q values between 0.1 and 0.2 using amplitude modulation method. As seen from the simulation results, the former is better; it removes all the high q ions. The latter only removes part of the high q ions.

2.5.2. *High mass reject filter and mass filter with small stability islands*

The configuration of Q1 working as a high mass reject filter and Q2 as a mass filter with small stability islands is shown in Fig. 7(b). Detailed transmission curve of Q2 is described in 2.3 and 2.4. Again, we assume $\alpha = V2/V1$ keeps constant in mass scanning. V1 and V2 are the amplitudes of the main driving RF of Q1 and Q2, respectively. The q value of the stable ions running through Q1 varies with α value. If $\alpha = q2/q1$, it is expected to received a mass peak with $R_{0.1} = 1150$ according to Fig. 5. The resolution reaches 1150 when $q' = 0.19$, which stays constant at short separation time $n = 30$ and 40 (Fig. 5). When α increases from q2/q1 to q3/q1, the resolution increases at the cost of sensitivity; similar experimental results have been reported [12].

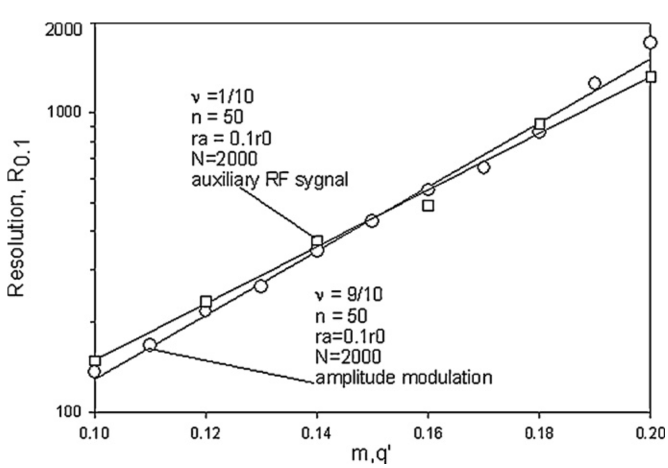

Fig. 8. Dependences of resolution $R_{0.1}$ on excitation parameter q' and modulation parameter m (given in log scale).

In auxiliary quadrupole excitation (Fig. 4), the resolution of the stability islands is improving with increasing q' at the cost of sensitivity. The small dips at the peaks of $q' = 0.10$ and 0.12 may be caused by quadrupole excitations. The resolution reaches 1150 when $q' = 0.19$, which stays constant at short separation time $n = 30$ and 40 (Fig. 5). Similar phenomena are found in amplitude modulation (Fig. 6). From Fig. 8 we can see that the resolution power $R_{0.1}$ in log scale depends linearly on the q' and m values. Both quadrupole excitations and auxiliary quadrupole excitation could improve resolution, and from numeric simulation alone it is difficult to tell which is better.

3. Results and discussion

A tandem RF-only quadrupole mass filter consisting of two short quadrupole rod sets is proposed and studied by computer simulations in this study. For RF reject mass filter Q1, the auxiliary RF voltage with parameters $\nu = 1/10$ and $q' = 0.02–0.06$ may be used. In this setting, high mass ions with q values equal to 0–0.2 are removed. For amplitude modulation with parameters $\nu = 9/10$ and $m = 0.1–0.25$, high mass ions with q values equal to 0.1–0.2 are removed. According to simulation results, Q1 is an efficient high mass ions rejecter and it only needs $n = 40–50$ RF cycles.

Auxiliary quadrupole excitation and amplitude modulation also produce small stability islands near $q = 0.908$, and the resolution power $R_{0.1}$ of the stability island in log scale depends linearly on the q' and m values.

Two configurations of tandem RF-only quadrupole mass filters are presented here. High mass reject filter is added before axial ion excitation mass filter and mass filter with small stability islands. In both configurations, the background noise could be reduced and the performance of the main mass filter Q2 improved by the mass shift between Q1 and Q2.

This numeric simulation is quite elementary. Quite a few problems, in particular the relations between mass and phase shift between Q1 and Q2, need to be further investigated using both simulation and experiments, and there very likely exists an optimal phase difference between the two mass filters to let pass most of the stable ions.

Acknowledgments

N.V. Konenkov thanks the Department of Chemistry of Fudan University for funding his visit. This work was supported by the China Natural Science Foundation (20527004) and the Science and Technology Commission of Shanghai Municipality (08DZ2270500).

References

[1] P.H. Dawson (Ed.), Quadrupole Mass Spectrometry and Its Applications, American Institute of Physics, 1995, originally published by Elsevier, New York, Amsterdam, 1976.
[2] U. Brinkmann, A modified quadrupole mass filter for the separation of ions of higher masses with high transmission, Int. J. Mass Spectrom. Ion Phys. 9 (1972) 161.
[3] J.A. Richards, R.M. Huey, J.A. Hiller, A new operating mode for the quadrupole mass filter, Int. J. Mass Spectrom. Ion Process. 12 (1973) 317–339.
[4] A.E. Holme, Operation of a quadrupole mass filter with only an R.F. voltage component applied to the rod system, Int. J. Mass Spectrom. Ion Process. 22 (1976) 1–5.
[5] A.E. Holme, S. Sayyid, J.H. Leck, A detailed study of the quadrupole mass filter operating with no DC component of the rods, Int. J. Mass Spectrom. Ion Process. 26 (1976) 191–204.
[6] J. Yang, J.H. Leck, Operation of the quadrupole mass-spectrometer in the ac mode, Vacuum 32 (1982) 691–694.
[7] D.N. Ross, J.H. Leck, A novel quadrupole mass spectrometer operating with no dc voltage component on the rods, Int. J. Mass Spectrom. Ion Process. 49 (1983) 1–9.
[8] J. Yang, J.H. Leck, The operation of a novel quadrupole mass spectrometer in hostile atmospheres, Int. J. Mass Spectrom. Ion Process. 60 (1984) 127–136.

[9] F.A. Londry, J.W. Hager, Mass selective axial ion ejection from linear ion trap, J. Am. Soc. Mass Spectrom. 14 (2003) 1130–1147.
[10] J.W. Hager, Performance optimization and fringing field modifications of a 24-mm long RF-only quadrupole mass spectrometer, Rapid Commun. Mass Spectrom. 13 (1999) 740–748.
[11] J.W. Hager, A new linear ion trap mass spectrometer, Rapid Commun. Mass Spectrom. 16 (2002) 512–526.
[12] Z. Du, D.J. Douglas, A novel tandem quadrupole mass analyzer, J. Am. Soc. Mass Spectrom. 10 (1999) 1053–1066.
[13] M.U. Sudakov, N.V. Konenkov, D.J. Douglas, T. Glebova, Excitation frequencies of ions confined in a quadrupole field with quadrupole excitation, J. Am. Soc. Mass Spectrom. 11 (2000) 11–18.
[14] N.V. Konenkov, L.M. Cousins, V.I. Baranov, M.U. Sudakov, Quadrupole mass filter operation with auxiliary quadrupolar excitation: theory and experiment, Int. J. Mass Spectrom. 208 (2001) 17–27.
[15] N.V. Konenkov, M.U. Sudakov, D.J. Douglas, Matrix methods for the calculation of stability diagrams in quadrupole mass spectrometry, J. Am. Soc. Mass Spectrom. 13 (2002) 597–613.
[16] N.V. Konenkov, A.N. Korolkov, M. Makhmudov, Upper stability island of the quadrupole mass filter with amplitude modulation of applied voltage, J. Am. Soc. Mass Spectrom. 16 (2005) 379–387.
[17] Q. Song, S.A. Smith, L. Gao, Mass selection of ions from beams using waveform isolation in radiofrequency quadrupoles, Anal. Chem. 81 (2009) 1833–1840.